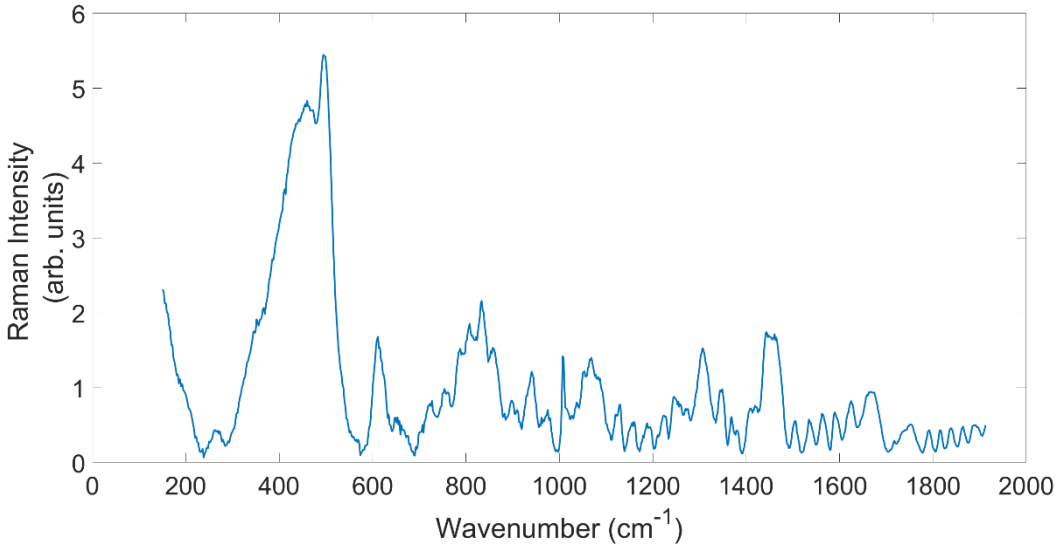

Supplementary Fig. 1: a) average baselined bovine cheek spectra taken with 830.0 nm excitation and needle probe #1. Acquisition time = 15x20s.

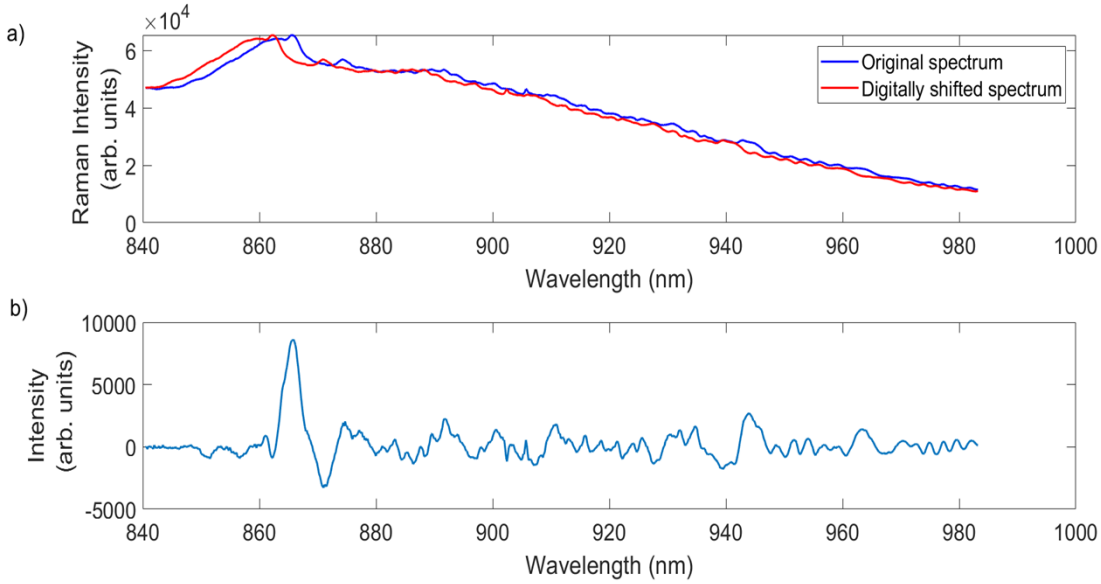

Supplementary Fig. 2: a) average bovine cheek spectra, plus a digitally shifted (by 3.35 nm) version. b) resulting 'difference spectrum' obtained using previously described k factor plus median filter methods. Acquisition time = 15x40s.

Supplementary Figure 2 demonstrates the technique of digitally shifting a spectrum and then calculating a difference spectrum. This calculation was performed on the 830.0 nm bovine cheek data shown in the main manuscript in Fig 4a). The digital offset applied to the data was 3.35 nm, which is the obtained spectral distance between peaks in the two spectra shown in Fig 4a), rather than 2.4 nm which is the *excitation difference* between the two laser wavelengths used to obtain the measurements. Subsequent to digital shifting, the two spectra were k factor normalised and mean centered using the median filter method described in 'Experimental Methods – SERDS Setup' within the main text. It is clear from comparing the resulting difference spectrum in Supplementary Fig 2a) to the actual SERDS difference spectrum in Fig 4b), that the 'digitally shifting'

technique does not remove the etaloning contributions from the spectra, and that the quality of the Raman data is degraded as compared to the SERDS technique.

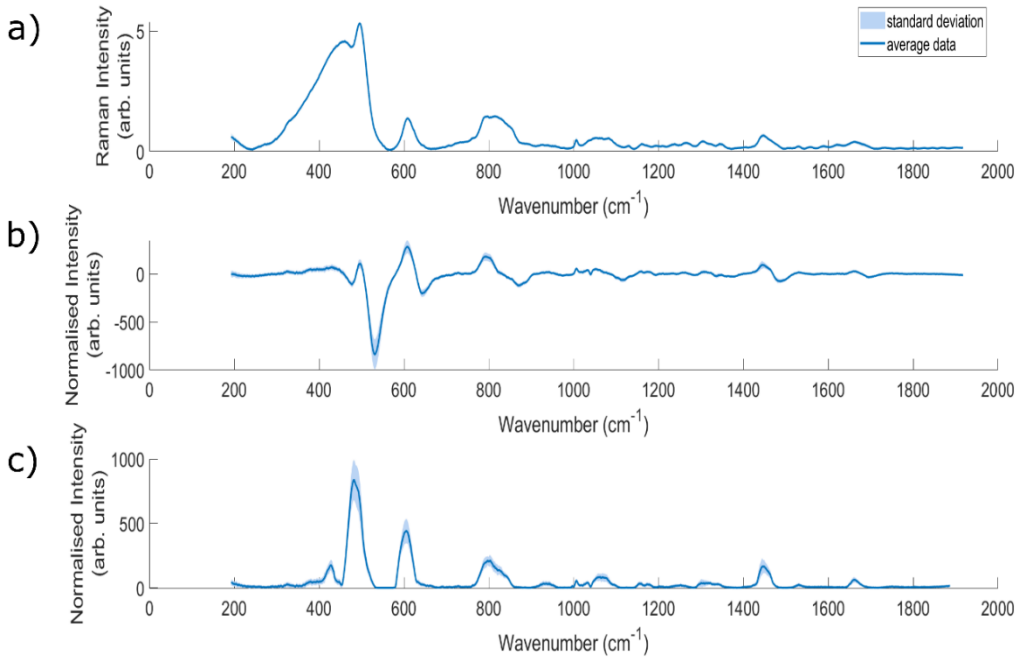

Supplementary Figure 3: average a) standard Raman, b) SERDS difference and c) SERDS reconstructed spectra from the cancerous lymph node measured. Acquisition time standard Raman spectra = 20s. Acquisition time SERDS spectra = (10s – 10s). Standard deviation is indicated by shaded region, for sub figure a) this is too small to be visible.

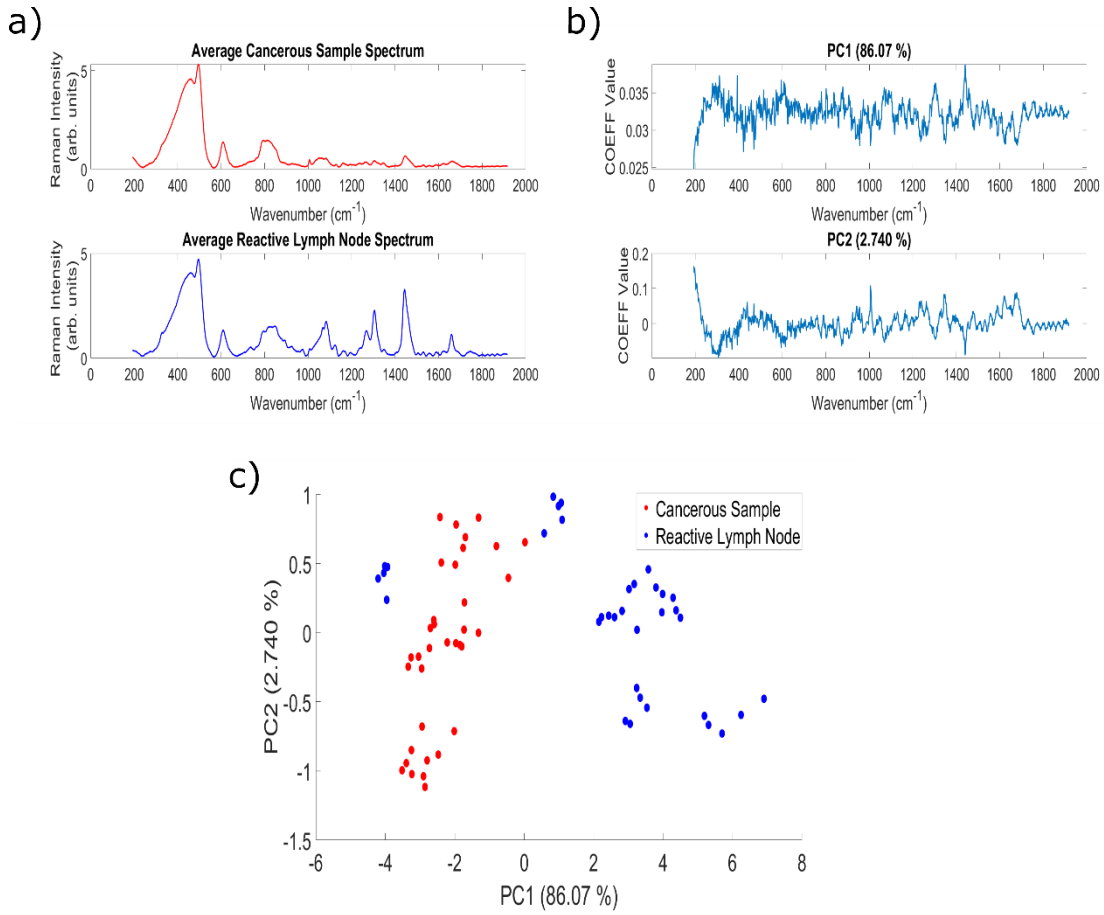

Supplementary Figure 4: For the standard Raman spectra: a) average spectra of the cancerous sample and reactive lymph node sample b) Loadings plots for most discriminating principal components c) corresponding PC SCORES plot. Acquisition Time = 40s.

The PCA data for the standard Raman spectra of the lymph nodes can be seen in Supplementary Figure 4. Both etaloning and silica signals clearly seen within the average spectra of each pathology type (Supplementary Figure 4a)); although the etaloning signals are most obvious within the reactive lymph node data. Supplementary Figure 4b) demonstrates that etaloning signals feature prominently in both of the most statistically significant PCs, which indicates that variation in the etaloning pattern is a major contribution to the variation in the data set.

The scores plot in Supplementary Figure 4c) shows that a statistical separation between pathologies is achieved, although there is a large spread across the reactive lymph node spectra scores values. This could be related to the two different "types" of reactive lymph node spectra demonstrated within Figure 7. The corresponding p value for this separation is 1.4768×10^{-11}.

The corresponding SERDS reconstructed spectra data can be seen in Supplementary Figure 4. The average spectra (Supplementary Figure 5a)) have no visually apparent etaloning contributions, and a significant reduction to the broad silica background region (although two sharp silica peaks are still present). This is reflected in the PCs, demonstrated in Supplementary Figure 5b). The main difference between the two seems to be a difference in intensity for the two silica peaks, however both contain clear chemical signals originating from within the samples, and no apparent etaloning contributions. The resulting scores plot in Supplementary Figure 5c) provides a clearer separation than was achieved with the standard Raman spectra, and corresponds to a p-value of 1.8069×10^{-16}, which confirms the improved statistical strength of the separation.

These simple PCA comparisons indicate that the use of the SERDS reconstructions provides a stronger statistical separation between the two pathologies within the data set than conventional spectra taken using the Raman needle probe #2. Most importantly, the use of the SERDS spectra removes the presence of etaloning

from within the most significant principal components, indicating that the highest levels of variation originate instead from chemical changes from within the sample.

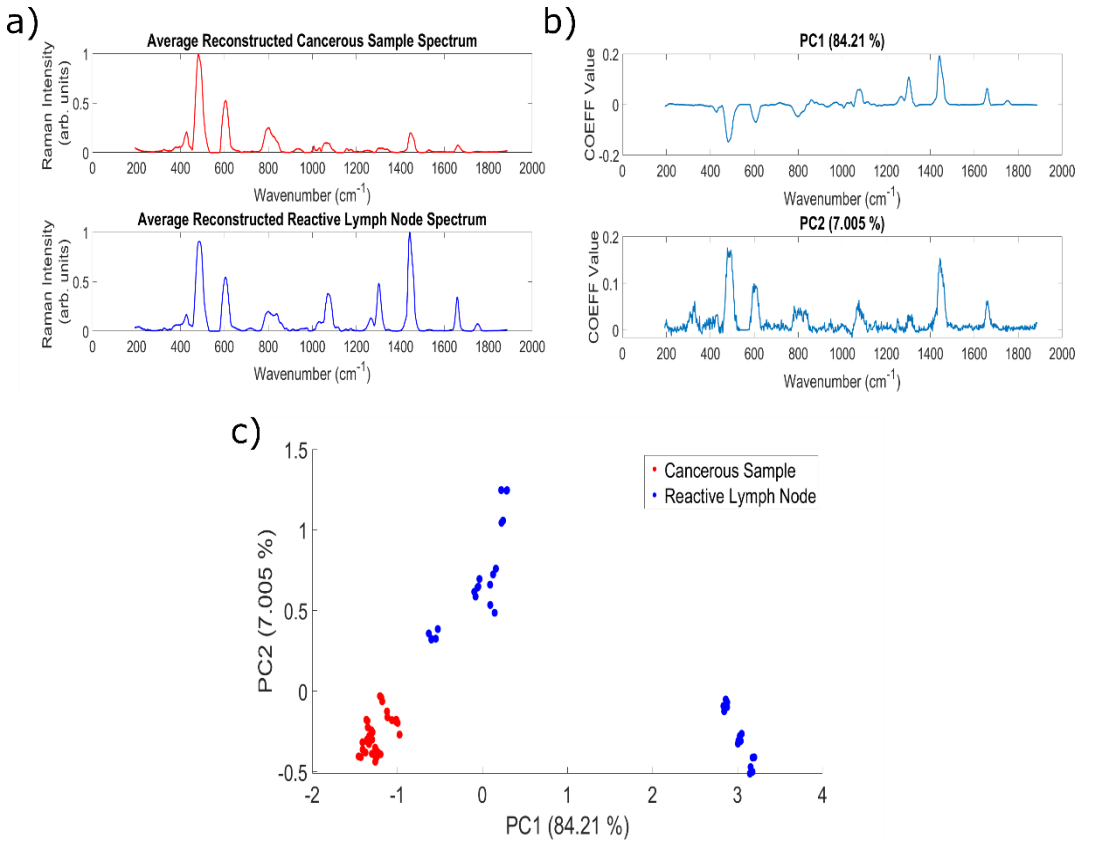

Supplementary Figure 5: For the reconstructed SERDS spectra: a) average spectra of the cancerous sample and reactive lymph node sample b) Loadings plots for most discriminating principal components c) corresponding PC SCORES plot. Acquisition Time = (20s – 20s).

This trend is replicated by the use of the SERDS difference spectra, shown in Supplementary Figure 6, achieving a p-value of 1.85×10^{-13} and demonstrating no visible etaloning signals within either of the most significant principal components. It has been reported within the literature that the transformation of difference spectra into reconstructed Raman spectra has the potential to introduce artefacts into the spectra[48]. However, given that both the SERDS difference and reconstructed methods offer increased statistical separation of the spectra and remove etaloning as a primary source of variation within the dataset, these results confirm that the use of either type of SERDS spectra results in an improvement to data quality in terms of fluorescence and etaloning spectral contributions.

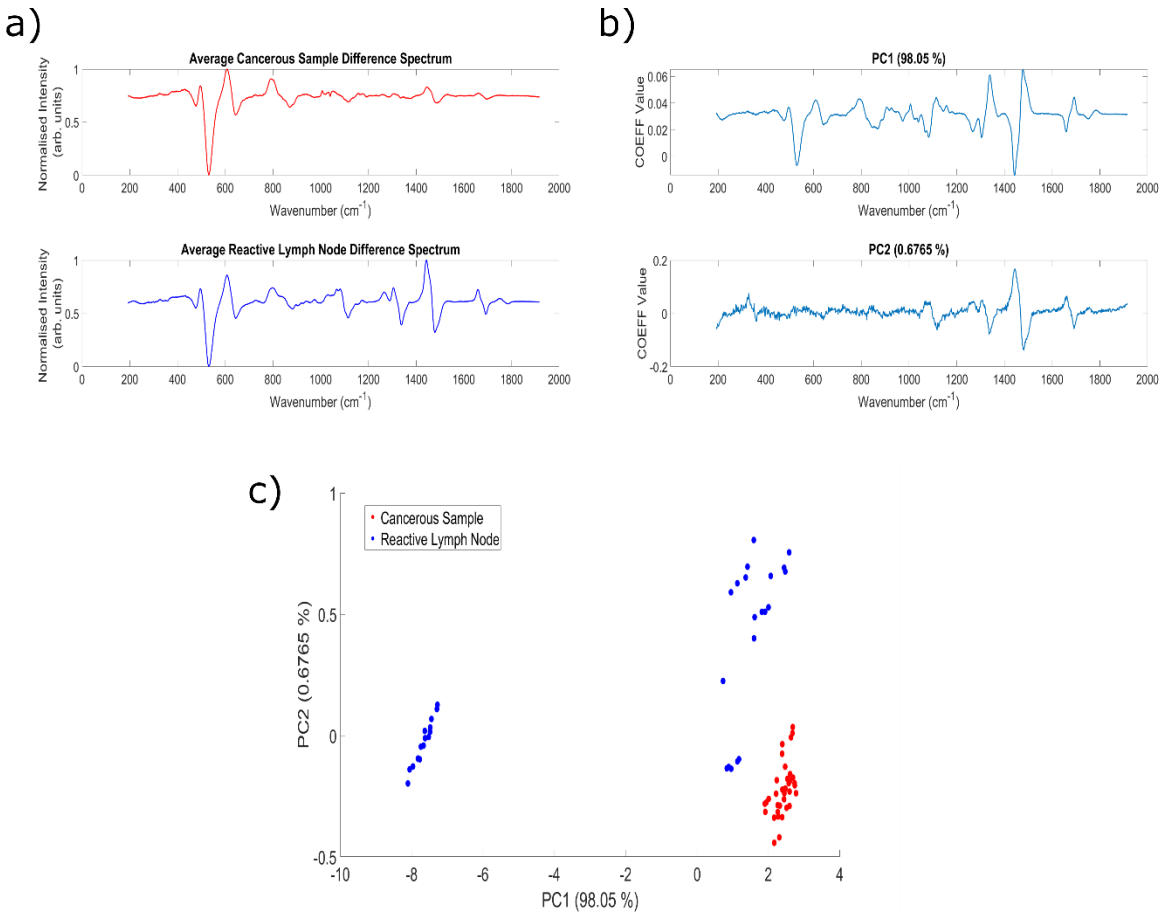

Supplementary Figure 6: For the SERDS difference spectra: a) average spectra of the cancerous sample and reactive lymph node sample b) Loadings plots for most discriminating principal components c) corresponding PC SCORES plot. Acquisition Time = (20s – 20s).